ExoSensor 517: A Dual-Analyte Fluorescent Chemosensor for Visualizing Neurotransmitter Exocytosis

Jessica L. Klockow, Kenneth S. Hettie, and Timothy E. Glass*

Department of Chemistry, University of Missouri—Columbia, 601 South College Avenue, Columbia, Missouri 65211, United States

S Supporting Information

ABSTRACT: A dual-analyte fluorescent chemosensor (ExoSensor 517) for the direct visualization of neurotransmitters released upon exocytosis is presented. The sensor exploits the high concentration of neurotransmitters (e.g., glutamate, norepinephrine, and dopamine) and the pH gradient between the vesicle and synaptic cleft. The cooperative recognition elements require both binding and a change in environmental pH to afford a fluorescence response which makes ExoSensor 517 one of the first integrated molecular logic gates to be used for biological applications.

KEYWORDS: chemosensor, neurotransmitter, logic gate, exocytosis, fluorescence
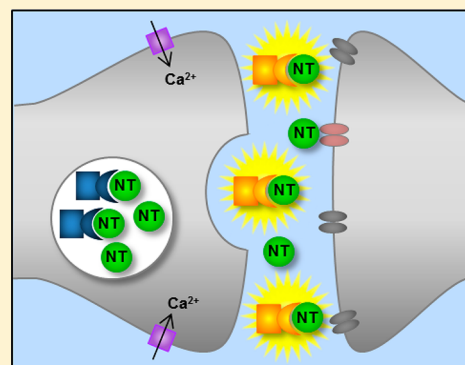
Neurotransmitters are critical to the regulation of the central and peripheral nervous systems and command a number of functions such as learning, memory, sleep, and movement.[1,2] Discerning the machinery involved in vesicular fusion, the spatiotemporal mechanisms of synaptic release, and the chemical activity of neurotransmitters is vital to understanding both normal and atypical cellular processes. The ability to effectively monitor exocytotic operations bolsters research in neuroscience, serving as a useful tool in the study of neurophysiology and neuropsychiatric disorders. Methods to evaluate exocytosis include fluorescence imaging,[3−7] capillary electrophoresis,[8−11] microelectrochemistry,[12,13] and mass spectrometry.[14] Nonoptical techniques are limited by poor throughput and a lack of spatial resolution.[15] Conversely, fluorescence methods offer a sensitive means to elucidate the spatial distribution of neuronal vesicles and chemical messengers.

Fluorescence imaging of secretion was studied early on by loading chromaffin cells with acridine orange and observing a loss in fluorescence upon exocytosis.[4] More recently, exocytosis has been visualized using the genetically encoded synapto-pHluorins, wherein a pH-sensitive GFP construct is expressed on the inner membrane of secretory vesicles. The engineered vesicles fluoresce upon exocytosis due to a change in pH from the acidic synaptic vesicle ($\sim$5) to the neutral synaptic cleft ($\sim$7.4).[5] These methods solely monitor the process of vesicle membrane fusion during an exocytotic event but do not directly image active neurotransmitters released upon exocytosis. In recent years, a genetically encoded CFP/YFP FRET biosensor was developed to monitor glutamate release, spillover, and reuptake by fluorescence.[16] However, these protein-based biosensors require genetic manipulation and display high,

irreversible affinity for glutamate with limited dynamic range and overall small changes in fluorescence. To avoid the use of protein-based fluorophores, a pH-sensitive fluorescent false neurotransmitter (FFN) has been developed to monitor exocytosis. This fluorescent tracer is loaded into vesicles expressing VMAT and fluoresces upon exocytosis similar to the synapto-pHluorins.[17]

We recently developed NeuroSensor 521 (NS521) as a fluorescent chemosensor for selective labeling and imaging of the neurotransmitters norepinephrine and dopamine inside secretory vesicles (Figure 1).[18] The sensor enters the vesicle
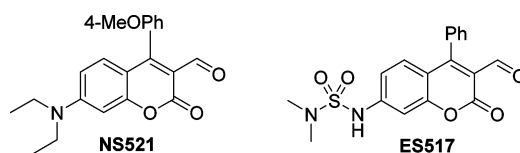

Figure 1. Structures of NS521 and ES517.

and binds to the primary amine of the catecholamine, creating a positively-charged iminium ion. The charged complex cannot translocate across the vesicular membrane and becomes trapped, accumulating inside the vesicle. Formation of the iminium ion also induces a bathochromic shift in absorbance that can be selectively excited at 488 nm allowing the neurotransmitter to be imaged directly, giving the signature punctate fluorescence. To image exocytosis of these neuro-

transmitters, we sought to create a pH-sensitive sensor based on the NS521 model.

Herein, we report an approach that utilizes a novel dual-analyte chemosensor, ExoSensor 517 (ES517), that selectively labels primary amine neurotransmitters found at high concentrations within vesicles (e.g., glutamate, norepinephrine, and dopamine) and allows for direct visualization of only active neurotransmitters released upon exocytosis by capitalizing on the pH gradient between the vesicle and the synaptic cleft. ES517 incorporates two distinct recognition elements into a single molecular receptor and requires both analyte binding and pH change to afford strong fluorescence at 517 nm. The logic gate design strategy allows for direct imaging of released neurotransmitters while minimizing interference with native neurotransmitter trafficking due to the reversible recognition motif. To our knowledge, this is the first integrated molecular logic gate for biological applications.

As depicted in Figure 2, the dual-analyte sensor can enter the vesicle and selectively bind to primary amine neurotransmitters at high concentrations, yet remain fluorescently "off" due to the acidic environment. Formation of a positively-charged complex

causes the bound sensor to become trapped within the vesicle, encouraging sensor accumulation. Exocytosis releases the bound sensor complex into the synaptic cleft and the change in environmental pH switches the fluorescence "on" for only the released sensor in its bound state.

To create a sensor that would respond in this way, the diethyl amino group of NS521 was exchanged for an electron-poor sulfamide that can be deprotonated at neutral pH to become electron-rich (Scheme 1). The sensor fluoresces via an

Scheme 1. Neurotransmitter Binding and Deprotonation of ES517[a]

Φ_{fl} = 0.0043 (A) Φ_{fl} = 0.0032 (B)
Φ_{fl} = 0.0039 (C) Φ_{fl} = 0.0030 (D)
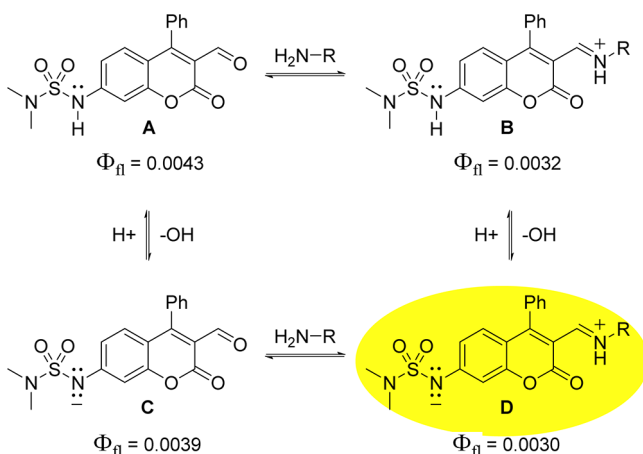
[a]Quantum yields were measured in triplicate in buffer (50 mM bis-tris propane, 120 mM NaCl, 1% DMSO) alone (A and C) and with saturating glutamate (300 mM, B and D) at pH 5.0 (A and B) and 7.4 (C and D). Excited at 488 nm. Calculated by using fluorescein as a fluorescence standard (Φ_{fl} = 0.850).
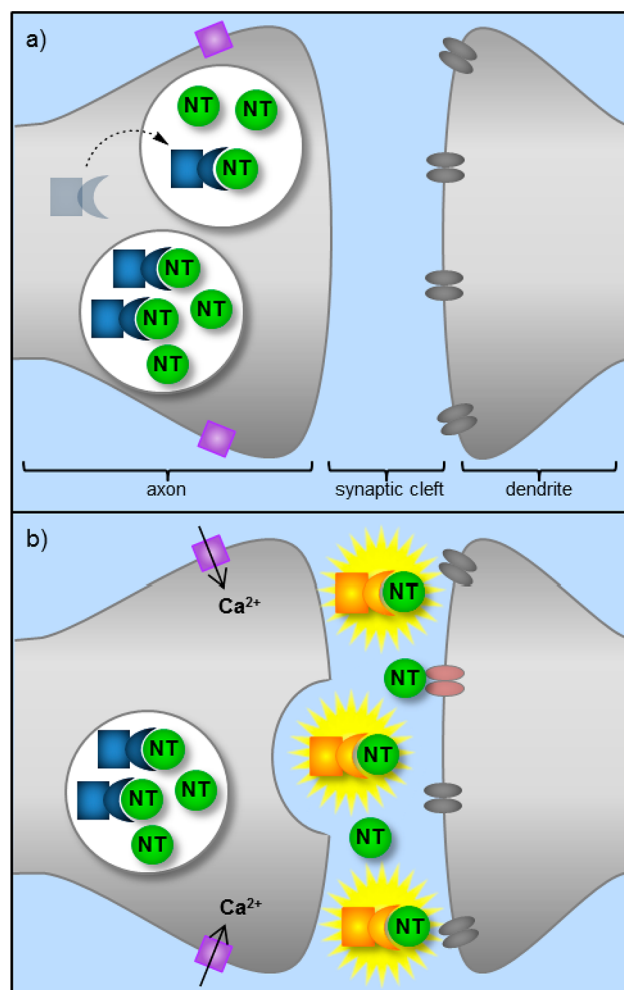
Figure 2. Sensing mechanism of ES517. (a) Sensor enters vesicle and selectively labels the neurotransmitter (NT). The bound complex accumulates and fluorescence is "off" due to low pH (5). (b) Influx of Ca^{2+} triggers exocytosis. The increase in environmental pH in the synaptic cleft (7.4) switches the fluorescence "on" for only the bound complex.

intramolecular charge transfer (ICT) state in which the sulfamide acts as an electron donor and the aldehyde acts as an electron acceptor. Both analyte binding and sulfamide deprotonation enhance the charge transfer across the fluorophore. Since binding to the analyte and deprotonation of the sensor both produce large bathochromic shifts, exciting the sensor at the highest wavelength of absorption will allow visualization of only the active neurotransmitters in the synapse. Any unbound sensor molecules would not be visualized as they absorb at much lower wavelengths.

In the cytosol, ES517 (A) will exist largely in the deprotonated form (C) due to the neutral pH and relatively low concentration of amines. Both forms A and C would have weak fluorescence as they lack the iminium ion as a strong acceptor. When ES517 enters the vesicle, it binds to the neurotransmitter due to its high concentration producing the iminium ion B. Form B would have marginal electron transfer and weak fluorescence since the protonated sulfamide is a weak donor. Upon exocytosis, the bound complex enters the synaptic cleft, becomes deprotonated (structure D), and produces a marked fluorescence increase due to the enhanced ICT.

This mechanism of action is similar to that of known molecular logic gates;[19,20] however, this approach is distinct in that it integrates the switch, fluorophore, and receptor into one unit for the purposes of biological chemical sensing. To obtain the maximum fluorescence increase upon exocytosis, the sensor pK_a must be between the pH of the vesicle (5) and the synaptic cleft (7.4). The sulfamide functional group was chosen as

literature precedent indicated the pK_a would be approximately 6.[21]

ES517 was prepared in four steps (Scheme 2). Compound **1** was synthesized from commercially available starting materi-

Scheme 2. Synthesis of ES517
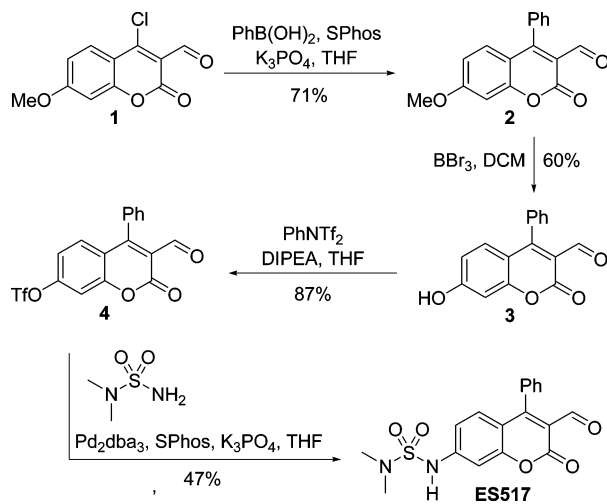
als[22] and underwent a Suzuki coupling to achieve the phenyl-substituted compound **2**. Demethylation and triflation of the resulting phenol produced compound **4**. The sulfamide substituent was appended using Buchwald-Hartwig coupling conditions to produce ES517.

ES517 was studied via UV/vis and fluorescence spectroscopy. Initially, binding studies were performed by titrating ES517 with glutamate and exciting at 488 nm, a region that is sufficiently red to prohibit absorbance and subsequent emission from the unbound sensor (Figure 3). A 12-fold fluorescence enhancement was obtained upon binding to glutamate though with a low binding constant ($K_a = 8.6 \ M^{-1}$). While low, this binding constant is actually preferred for reversible binding to the high millimolar concentration of glutamate in a vesicle (~300 mM).[23−25]

To test the pK_a of the bound sensor, ES517 was saturated with glutamate and the spectroscopic properties measured over a wide pH range (Figure 4). The protonated form of the bound sensor (Figure 2, structure B) absorbed at 368 nm. Upon deprotonation, two bands were observed at 428 and 458 nm. The 428 nm band was assigned to the unbound deprotonated form of the sensor (structure C, compare with Figure S1 in the Supporting Information). The 458 nm band therefore represents the bound, deprotonated sensor (structure D). The plot of pH vs intensity was fit to a pH isotherm, and the pK_a determined to be 6.3. The fluorescence quantum yield (Φ_{fl}) for ES517 was determined in each state using glutamate as the analyte (shown in Scheme 1). The quantum yields were similar, with the bound states being slightly lower than the unbound states. Since the sensor is selectively excited at a wavelength at which only form D absorbs, these quantum yields are sufficient for imaging purposes.

A pH titration of ES517 alone gave a pK_a of 6.3, indicating that formation of the iminium ion does not alter the sulfamide pK_a (Figure S1, Supporting Information). To verify that the spectroscopic changes observed were not due to deprotonation of the iminium ion, a control test using compound **2** was performed (Figure S7, Supporting Information). Compound **2**
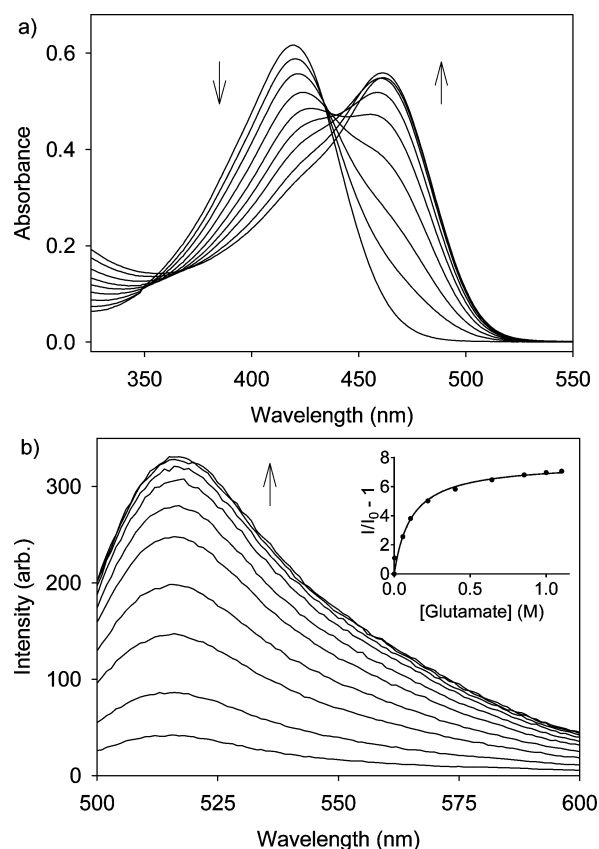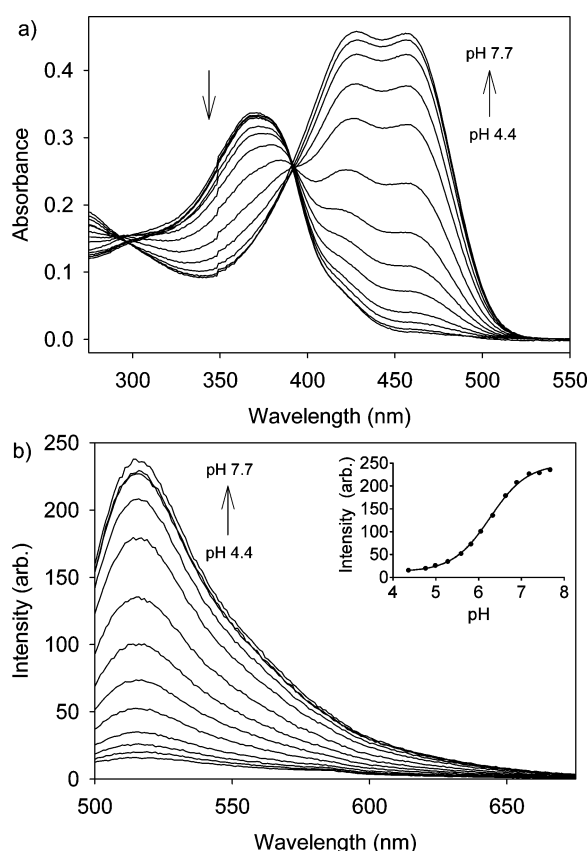
Figure 3. (a) Absorbance and (b) fluorescence titration of ES517 (20 μM) in buffer (50 mM bis-tris propane, 50 mM $Na_2S_2O_3$, 1% DMSO, pH 7.4) adding 20−800 μL aliquots of 1.5 M glutamate. $\lambda_{ex} = 488$ nm. Inset is the fit to a binding isotherm.

was saturated with glutamate, and the resulting iminium ion had a pK_a of ~9. This result indicates that the imine formed upon binding to the neurotransmitter will be protonated within the physiological pH ranges described.

To estimate the response of the sensor−glutamate complex to exocytosis, its fluorescence at pH 7.4 was compared to that at pH 5.0 and a 12-fold difference was calculated. This implies that the sensor−glutamate complex will produce a significant fluorescence enhancement upon exocytosis.

The key spectroscopic properties of ES517 binding to glutamate are tabulated in Table 1 along with several other neurotransmitters. As with the non-pH-sensitive NS521, all primary amine neurotransmitters bound relatively weakly with a preference for aromatic neurotransmitters. By contrast, the non-aromatic neurotransmitters produced the largest change in fluorescence upon binding at pH 7.4 due to the absence of PET quenching effects from the electron-rich aromatic groups. Importantly, all nonaromatic neurotransmitters produced large fluorescence increases upon pH change from 5.0 to 7.4. The catecholamines gave smaller, but still significant fluorescence increases and serotonin was unique in that it gave little fluorescence change (Figure 5).

In summary, ExoSensor 517, a dual-analyte fluorescent chemosensor, was developed for the visualization of neurotransmitters released upon exocytosis. The logic-based design strategy exploits high vesicular neurotransmitter concentrations and the pH gradient between the vesicle and synaptic cleft. The glutamate-bound sensor afforded a 12-fold fluorescence enhancement to conditions mimicking synaptic release, and

C

dx.doi.org/10.1021/cn400128s | ACS Chem. Neurosci. XXXX, XXX, XXX−XXX

Figure 5. Fluorescence enhancements of ES517 saturated with various amine analytes under pH conditions simulating exocytosis.

■ ASSOCIATED CONTENT

ⓢ Supporting Information

Spectroscopic parameters, experimental procedures, and NMR spectra. This material is available free of charge via the Internet at http://pubs.acs.org.

■ AUTHOR INFORMATION

■ ACKNOWLEDGMENTS

■ REFERENCES

(1) Deng, Y.-H., Wang, H., and Zhang, H.-S. (2008) Determination of amino acid neurotransmitters in human cerebrospinal fluid and saliva by capillary electrophoresis with laser-induced fluorescence detection. *J. Sep. Sci. 31*, 3088−3097.

(2) Boyd, B. W., Witowski, S. R., and Kennedy, R. T. (2000) Trace-level amino acid analysis by capillary liquid chromatography and application to in vivo microdialysis sampling with 10-s temporal resolution. *Anal. Chem. 72*, 865−871.

(3) Gubernator, N. G., Zhang, H., Staal, R. G., Mosharov, E. V., Pereira, D. B., Yue, M., Balsanek, V., Vadola, P. A., Mukherjee, B., Edwards, R. H., Sulzer, D., and Sames, D. (2009) Fluorescent false neurotransmitters visualize dopamine release from individual pre-synaptic terminals. *Science 324*, 1441−1444.

(4) Steyer, J. A., Horstmann, H., and Almers, W. (1997) Transport, docking and exocytosis of single secretory granules in live chromaffin cells. *Nature 388*, 474−478.

(5) Miesenböck, G., De Angelis, D. A., and Rothman, J. E. (1998) Visualizing secretion and synaptic transmission with pH-sensitive green fluorescent proteins. *Nature 394*, 192−195.

(6) Felmy, F. (2007) Modulation of cargo release from dense core granules by size and actin network. *Traffic 8*, 983−997.

(7) Burchfield, J. G., Lopez, J. A., Mele, K., Vallotton, P., and Hughes, W. E. (2010) Exocytotic vesicle behavior assessed by total internal reflection fluorescence microscopy. *Traffic 11*, 429−439.

(8) Kennedy, R. T., Oates, M. D., Cooper, B. R., Nickerson, B., and Jorgenson, J. W. (1989) Microcolumn separations and the analysis of single cells. *Science 246*, 57−63.

Figure 4. (a) Absorbance and (b) fluorescence pH titration of ES517 (20 μM) with 300 mM glutamate in buffer (50 mM bis-tris propane, 120 mM NaCl, 1% DMSO) adjusting the pH from 4.4 to 7.7. λ_{ex} = 488 nm. Inset is the fit to a pH isotherm.

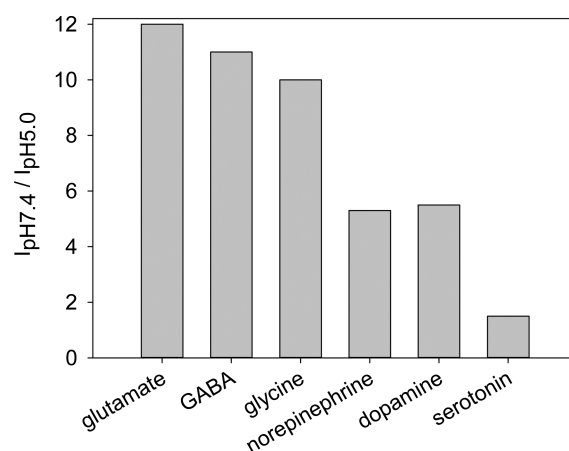### Table 1. Binding and Spectroscopic Properties of ES517 with Various Primary Amine Neurotransmitters

neurotransmitter[a]	K_a (M^{-1})	I_{sat}/I_0[b]	$I_{pH7.4}/I_{pH\,5}$[c]
glutamate	8.6	12	12[d]
GABA	8.3	27	11[d]
glycine	9.2	25	10[d]
norepinephrine	49	14	5.3[e]
dopamine	55	10	5.5[e]
serotonin	54	0.5	1.5[e]

[a]Binding studies of ES517 (20 μM) with saturating amounts of analyte in buffered conditions (50 mM bis-tris propane, 50 mM Na$_2$S$_2$O$_3$, 1% DMSO, pH 7.4) with ±10% error based on triplicate titration. [b]Fluorescence enhancement upon binding analyte at pH 7.4 (I_{sat} taken from the theoretical max of the binding isotherm). λ_{em} = 517 nm. [c]Ratio of fluorescence at pH 7.4 vs 5.0 of ES517 (20 μM) saturated with analyte. [d]Saturated with 300 mM analyte. [e]Saturated with 100 mM analyte.

further studies are underway to optimize the fluorescence response to quenching analytes. ES517 serves as a potential research tool for studying the mechanisms underlying neuro-transmission. Biological testing of ES517 will be pursued in due course, and special considerations will include validating sensor uptake, assessing the rate of clearance, and assessing the dissociation of the sensor complex.

D

dx.doi.org/10.1021/cn400128s | *ACS Chem. Neurosci.* XXXX, XXX, XXX−XXX

(9) Kristensen, H. K., Lau, Y. Y., and Ewing, A. G. (1994) Capillary electrophoresis of single cells: observation of two compartments of neurotransmitter vesicles. *J. Neurosci. Methods 51*, 183−188.

(10) Chang, H.-T., and Yeung, E. S. (1995) Determination of catecholamines in single adrenal medullary cells by capillary electrophoresis and laser-induced native fluorescence. *Anal. Chem. 67*, 1079−1083.

(11) Omiatek, D. M., Dong, Y., Heien, M. L., and Ewing, A. G. (2010) Only a fraction of quantal content is released during exocytosis as revealed by electrochemical cytometry of secretory vesicles. *ACS Chem. Neurosci. 1*, 234−245.

(12) Ponchon, J. L., Cespuglio, R., Gonon, F., Jouvet, M., and Pujol, J. F. (1979) Normal pulse polarography with carbon fiber electrodes for in vitro and in vivo determination of catecholamines. *Anal. Chem. 51*, 1483−1486.

(13) Leszcezyszyn, D. J., Jankowski, J. A., Viveros, O. H., Diliberto, E. J., Near, J. A., and Wightman, R. M. (1990) Nicotinic receptor-mediated catecholamine secretion from individual chromaffin cells. Chemical evidence for exocytosis. *J. Biol. Chem. 265*, 14736−14737.

(14) Li, L., Garden, R. W., and Sweedler, J. V. (2000) Single-cell MALDI: a new tool for direct peptide profiling. *Trends Biotechnol. 18*, 151−160.

(15) Ge, S., Koseoglu, S., and Haynes, C. L. (2010) Bioanalytical tools for single-cell study of exocytosis. *Anal. Bioanal. Chem. 397*, 3281−3304.

(16) Hires, S. A., Zhu, Y., and Tsien, R. Y. (2008) Optical measurement of synaptic glutamate spillover and reuptake by linker optimized glutamate-sensitive fluorescent reporters. *Proc. Natl. Acad. Sci. U.S.A. 105*, 4411−4416.

(17) Rodriguez, P. C., Pereira, D. B., Borgkvist, A., Wong, M. Y., Barnard, C., Sonders, M. S., Zhang, H., Sames, D., and Sulzer, D. (2013) Fluorescent dopamine tracer resolves individual dopaminergic synapses and their activity in the brain. *Proc. Natl. Acad. Sci. U.S.A. 110*, 870−875.

(18) Hettie, K. S., Liu, X., Gillis, K. D., and Glass, T. E. (2013) Selective catecholamine recognition with NeuroSensor 521: a fluorescent sensor for the visualization of norepinephrine in fixed and live cells. *ACS Chem. Neurosci. 4*, 918−923.

(19) de Costa, M. D. P., de Silva, A. P., and Pathirana, S. T. (1987) Two dimensional fluorescent sensors: the different dependences of the fluorescence band position and the fluorescence quantum yield of 1,5-diphenyl-3-vinyl-Δ^2-pyrazoline upon solvent dipolarity and hydrogen bond acidity. *Can. J. Chem. 65*, 1416−1419.

(20) de Silva, A. P., and McClenaghan, N. D. (2004) Molecular-scale logic gates. *Chem.—Eur. J. 10*, 574−586.

(21) Wolfbeis, O. S., and Baustert, J. H. (1985) Synthesis and spectral properties of 7-(*N*-arylsulfonyl)aminocoumarins, a new class of fluorescent pH indicators. *J. Heterocycl. Chem. 22*, 1215−1218.

(22) Steinführer, T., Hantschmann, A., and Pietsch, M. (1992) Heterocyclish [c]-anellierte Cumarine aus 4-Azido-3-cumarincarbalde-hyden. *Liebigs Ann. Chem.*, 23−28.

(23) Schenck, S., Wojcik, S. M., Brose, N., and Takamori, S. A. (2009) A chloride conductance in VGLUT1 underlies maximal glutamate loading into synaptic vesicles. *Nat. Neurosci. 12*, 156−162.

(24) Riveros, N., Fiedler, J., Lagos, N., Muñoz, C., and Orrego, F. (1986) Glutamate in rat brain cortex synaptic vesicles: influence of the vesicle isolation procedure. *Brain Res. 386*, 405−408.

(25) Burger, P. M., Ehrenfried, M., Cameron, P. L., Maycox, P. R., Baumert, M., Lottspeich, F., De Camilli, P., and Jahn, R. (1989) Synaptic vesicles immunoisolated from rat cerebral cortex contain high levels of glutamate. *Neuron 3*, 715−720.